Int. J. Electrochem. Sci., 8 **(2013)** 8863 - 8892

International Journal of
ELECTROCHEMICAL
SCIENCE
www.electrochemsci.org

Review Paper

Developments of Immobilized Surface Modified Piezoelectric Crystal Biosensors for Advanced Applications

Sumit Pramanik[*], *Belinda Pingguan-Murphy, and Noor Azuan Abu Osman*

Department of Biomedical Engineering, University of Malaya, Kuala Lumpur - 50603, Malaysia
[*]E-mail: prsumit@gmail.com

Received: 16 October 2012 / *Accepted:* 29 April 2013 / *Published:* 1 June 2013

The development of biosensors has seen recent growth owing to their wide range of potential applications from the defending of bioterrorism to the detection of various diseases. Recent investigations in highly sensitive nanomaterials containing nanotechnology suggest the possibility of its advanced applications as biosensors in different biomedical fields. Besides highlighting the characteristic features of different classes of advanced biosensor across different fields of potential application, this article gives a clear overview of some specific investigations related to the surface immobilizations of piezoelectric biosensors employing effective materials and advanced technologies. Further, the current development of piezoelectric biosensors in the detection of potential biomolecules for advanced biomedical applications is critically reviewed. The qualitative and quantitative sensitivity of piezoelectric biosensors, various expressions of resonant frequency shift with changes in mass, thickness, density, and stress for piezoelectric materials are distinctly explored. The importance of several novel nanomaterials for the detection of various diseased biomolecules is clearly illustrated. This study concludes that proper selection of materials is potential to bring improvement in quality as well as reduction in cost of advanced biosensor devices.

Keywords: piezoelectric quartz crystal; immobilization; surface modification; nanotechnology; nanomaterial; biomaterial

1. INTRODUCTION

In recent years, an immense funding has been invested in the biomedical sectors and related industries as a direct result of the wide range of multi directional applications of biosensors [1]. During this period, there has been a notable progress in the application of nanomaterials particularly, in biosensors development, leading to numerous current prospects for the use of biosensors in the detection, monitoring, and medicinal diagnosis of biological molecules and diseases such as diabetes, cancer cell detection, and so on [2-5]. Besides their diagnostic medical applications, the biosensors

also permit the monitoring of artificial organs [6], sampling environmental pollutants for rapid and accurate monitoring [7], detection of food borne pathogens for quality appraisal [8, 9], and assessment of the potential danger of bioterrorism [10]. As a result, researchers from the fields, ranging from biomedical science to materials science engineering, have been undertaking to design, develop, and manufacture the new low-cost sensing devices for obtaining more efficient, accurate, rapid, and reliable information. The main fundamental factors related to development of conventional biosensors have been recognized. However, the handling of ceramic quartz crystals for various sensing applications, in practical terms, is still very difficult, owing to the conventional physical and analytical characteristics that result from a small size and fragile nature [11]. In this context, careful engineering of surface characteristics of a receptor based on composite materials (e.g., lead zirconate titanate (PZT)/polyvinylidene difluoride (PVDF), polar poly(γ-benzyl α,l-glutamate) (PBLG)/ poly(methylmethacrylate) (PMMA), etc) [12] can play major role in piezoelectric biosensors to detect the target molecules effectively without any difficulty of fragility [13]. However, selection of receptor materials and their proper surface properties in detection of a tiny specific biomolecule is one of the major challenges to the researchers to date. Thus, the primary goal of all the biosensor-researchers is to provide a continuous quantitative and qualitative analysis, thereby eliminating the time lag, whilst preserving the precision and accuracy of clinical analysis.

1.1. Purpose of this article

Past investigations on nano-biotechnology have confirmed that the nanomaterials with a high aspect ratio (i.e., length-to-diameter ratio) or a high specific surface area (i.e., surface-to-volume ratio) generally exhibit a significant improvement in sensitivity, as a result of higher electron transport phenomena. Surface modification through nanoparticles offers a tactic to achieve the advantages in the immobilization of biomolecular agents more precisely. However, no peer reviewed article has yet disclosed a detail study of surface modification techniques used in piezoelectric biosensors for advanced applications. Hence, we aims to present an overview of the recent developments in surface immobilization processes as applied to piezoelectric biosensors, using nanodetecting-materials for advanced biomedical applications. Therefore, the purpose of this article is not only to compare the advantages and functional characteristics of various biosensors in a wide field of novel applications, but to discuss some innovative technologies related to the new generation materials used for surface modification of piezoelectric crystals.

1.2. Chronology of biosensor developments

Whilst the first biosensor that is thought to be used at coal mine in 1911 to monitor gas leakage [14], the actual scientific profess of biosensor development was born after the publication of a paper on an electrochemical biosensor in 1953 by Professor Leland C. Clark Jr. Since then, scientists from various fields have been involved in trying to design and develop the different types of biosensor. A chronological development in biosensors is illustrated in Table 1.

Table 1. Chronology of biosensor developments

Year	Type of biosensor	Application	Reference
1911	Gas sensor	In coal mines since to monitor gas leakage	[14]
1916	Protein biosensor	On immobilization of proteins: adsorption of invertase on activated charcoal	[32]
1922	Glass pH electrode	Measurement of glass-surface potential	[33]
1952	First CO_2 gas sensor by Copenhagen	Measurement the blood gas carbon dioxide (Pco_2) tension	[34]
1953	Oxygen electrode	Recording of blood oxygen	[35]
1962	Amperometric electrode	Glucose detection	[36]
1964	First quartz crystal microbalance (QCM) sensor	Gas chromatography detector	[37]
1970	Ion selective Field Effect Transistor (ISFET) cribbed a fibre-optic sensor with immobilised ioxide or oxygen	Neurophysiological measurements	[38]
1973	Enzyme electrode based on amperometric (anodic) monitoring of liberated hydrogen peroxide (H_2O_2)	Determination of blood glucose	[39]
1975	First commercially produced glucose biosensor (model: 23YSI, make: Yellow Springs, USA)	Fast glucose assay in blood samples from diabetics	[40]
1975	First immunosensor	Detection and production of monoclonal antibody	[41]
1980	First fibre optic pH sensor	In-vivo blood gases	[42]
1982	First fibre optic-based biosensor for glucose	Glucose detection	[2]
1983	First surface plasmon resonance (SPR) immunosensor	Gas detection and biosensing	[43]
1984	First mediated amperometric biosensor	Glucose detection by using of ferrocene with glucose oxidase	[44]
1987	Blood-glucose biosensor (make: MediSense trade name ExacTech, Cambridge, USA)	To detect glucose in blood	[45]
1997	Neuronal biosensors	Neuro-sensing	[46]
2001	Ellipsometric biosensor	Nucleic acid detection	[47]

2004	Protein biosensors using fluorescence resonance energy transfer (FRET)	Studying live cell molecular event	[48, 49]
2005	Piezoelectric immunosensor	To detect the carcinoembryonic antigen	[50]
2007	Quantum dots biosensor	Cancer cell detection	[51]
2010	Biosensors of quantum dots, nanoparticles, nanowires, and nanotubes	Nanomedical applications	[52]
2011	Thin film transistor immunosensor	Detection of biochemicals such as enzymes, antibodies, DNA immobilization, and hybridization	[53]

1.3. Succinct perspectives of review articles on biosensors to date

The different perspectives of peer reviewed articles related to the development and application of biosensors are briefly summarised only to manifest the trends in the chronological progression from the beginning. In this context, Ivnitski *et al.* (1999) [8] had demonstrated the different physicochemical instrumental techniques, viz., infrared and fluorescence spectroscopy, flow cytometry, chromatography, and chemiluminescence, to detect the direct and indirect existence of pathogenic bacteria using different biosensors. Later, Vo-Dinh and Cullum (2000) [15] mentioned the progress of biochip systems in low-costs integrated circuit (IC) technology for biomedical applications. Wang (2001) [16] explained the principles and typical applications of glucose biosensors. Mulchandani *et al.* (2001) [17] described different biosensors that can detect organophosphate pesticides. Grayson *et al.* (2004) [18] gave an overview of the potential of a microfabrication technique, which is called as microelectromechanical system (MEMS), for the development of various sensors of biomedical application, including pressure sensors, and immunoisolation devices. Monk and Walt (2004) [19] described an immunoassay composed of optical fiber-based biosensors to increase the sensitivity, selectivity, selective reversibility, shelf life, and long-term stability. However, actual advancement of miniature fiber optic spectrophotometric instrumentation is yet to be commercialized. Again, Wang (2005) [20] has summarized the advanced progress of carbon nanotubes (CNTs) based electrochemical biosensors, particularly in amperometric (oxidase or dehydrogenase) enzyme electrodes and bioaffinity devices (e.g., DNA biosensors). Mohanty and Kougianos (2006) [21] mainly surveyed the different types of biosensor devices and their typical principles of operation. Li *et al.* (2006) [22] reviewed fluorescence resonance energy transfer (FRET) techniques for the application of protein biosensors. They, however, mentioned that the availability of good FRET pairs is one of the major challenges in FRET biosensor design. Then, Mok and Li (2008) [23] had focused on the development of aptamers in biosensors against various biomolecules by coupling aptamers to signal transducers for chemical and biological applications. The advanced aptamer technology uses the nucleic acids, which are fundamental molecules of life as research tools to enhance the understanding of physiological processes. This technology may be useful in drug discovery and the identification of infectious agents. Further, Yogeswaran and Chen (2008) [24] described the utility and typical advantages of nanowires

for biosensors development. Fan *et al.* (2008) [25] had focused on the progress of various optical biosensors (e.g., surface plasmon resonance (SPR), waveguides, fiber gratings, ring resonators, and photonic crystals) and their structures for label-free detection. However, they foresaw that a few levels of integration were still needed for advanced optical biosensor commercialization. Pohanka and Skládal (2008) [26] demonstrated electrochemical biosensors based on potentiometric, amperometric, and impedimetric biosensors and their commercial applications. Recently, Zhang *et al.* (2009) [27] have discussed some nanomaterials, including gold nanoparticles (GNPs), CNTs, and quantum dots (QDs), which can improve the mechanical, electrochemical, optical, and magnetic properties of biosensors. Garipcan et al. (2010) [14] brought attention mainly to the classification and historical nature of various biosensors. The design, unique features, and typical applications of various biosensors based on microbial cells were analyzed by Reshetilov *et al.* (2010) [28]. Shao et al. (2010) [29] had concluded that the electrodes of graphene based materials can show better unique properties (viz., specific electronic structure and superior performance in terms of electrocatalytic activity and macroscopic scale conductivity) than CNTs based biosensors for the detection of enzymes and other small biomolecules. This graphene is the building block of all dimensioned graphitic materials such as fullerene, CNTs, carbon nanofibers (CNFs), and graphite. They also mentioned that the doping of hetero atoms such as nitrogen or boron on graphene has not been done yet, although this might greatly affect sensor technology, as doped CNTs show better results than undoped CNTs. However, the synthesis process of graphene film itself and doping of hetero atoms is both tricky and complicated. Li *et al.* (2010) [30] had concluded that the GNP based optical, electrochemical, and piezoelectric based biosensors are able to show significantly improved performance in terms of sensitivity, long term stability, selectivity, and reliability. Furthermore, since the size of gold (Au) nanoparticles significantly affects the optical and electrical properties, the research on GNP and its nanostructured hybrids can display a unique feature in biosensor applications. However, the designing or developing of such a high order surface area of GNPs for a specific biosensor is a great challenge to researchers. Recently, Kumar M *et al.* (2011) [31] have reviewed some high aspect ratio materials, such as polymer nanowires, carbon nanotubes, and zinc oxide nanorods, which can promisingly improve the performance of biosensors. Depending on their report, the development of high performance-biosensors includes three stages: (a) synthesis of biomaterials (e.g., polypyrrole polymer, CNT, zinc oxide (ZnO), etc) into high aspect ratio nanostructures, (b) alignment of the nanostructures, and (c) immobilization of proteins.

2. SENSING PRINCIPLE AND CLASSIFICATION OF ADVANCED BIOSENSOR

The piezoelectric sensor depends on the piezoelectric effect, which was discovered by the Curie brothers in the late 19^{th} century. In piezoelectric effect, when a pressure (i.e., piezo in the Greek word) is applied to a piezoelectric material, it creates a mechanical deformation and a displacement of electrical charges. The change in electrical charges is resulted a piezoelectricity, which is highly proportional to the applied pressure. The sensing principle of biosensors basically depends on its field of applications. In general, a biosensor is an analytical device that is used mostly to detect and/or

monitor the target entities or analytes, including biological molecules, macromolecules, and elements [21]. Typically, a biosensor consists of three main components [14]: a *receptor* (i.e., a biological recognition part - responsible for the specific interaction with analyte via immobilized or probe molecules), a *transducer* (i.e., heart of the sensor - transduces the biological interaction into an electrical signal), and an *output system* (i.e., amplifier and display unit - visualizes the individual properties of a specific molecule in the analyte sample) (Figure 1). An *analyte* (i.e., target molecule) is a biological entity such as a biomolecule, macromolecule, protein, enzyme, antigen, nucleic acid (DNA or RNA), oligonucleotide, peptide nucleic acid (PNA), tissue, microbial entity, polysaccharide, or similar. These are attached to the receptors by chemical, physical or biological reactions. The analytes are complementary structures to the receptors such as antigen and antibody, metal ions and amino-acids, etc in a biosensor [14]. The two major functions of transducer are to detect the bio-signal of analyte and then, to convert the bio-signal into a corresponding electrical signal. The transferred electrical signals may be adequately amplified by an output system, and it finally, is viewed either on a digital panel of a suitable recorder or display unit. The output of an advanced biosensor mainly depends on the amplifying strategies, which can be modulated by biosensing elements such as impedance, intensity, and phase of electromagnetic (EM) radiation, electrical potential or voltage, current, and conductance, mass, temperature, and viscosity. Each of the sensing elements of the advanced biosensor can be modulated by advanced material technologies.

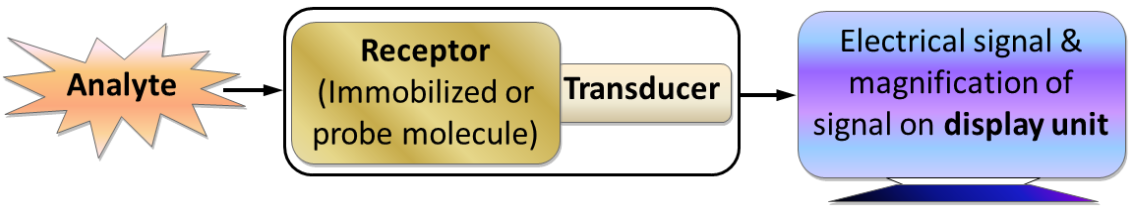

Figure 1. A general schematic diagram of different elements of a biosensor [21].

The key factors that affect the performance of an advanced biosensor are sensitivity, accuracy, calibration, background signal, hysteresis, long-term stability, dynamic response, and biocompatibility [54]. A sensor should be self-contained, perform in continuous monitoring (rather than make discrete measurements), and be reversible. The specific possible biolayers as bioreceptor molecules and molecular assemblages are important to know in terms of their structural integrity and signal generation, as illustrated in Table 2. The biosensors are generally classified based on their applications, sensor elements, biorecognition materials use, immobilization methods (on transducer surface), and transduction methods or transducing element. The specific possible biolayers capable of use as receptor molecules, and their corresponding structural integrity and output signal with complex hierarchy for molecular assemblages in biosensor applications, are illustrated in Table 3. Beside the conventional biosensors, the other advanced *in vivo* diagnostic based biosensors made of nanomaterials such as quantum dots [51, 55]. are used in magnetic resonance imaging (MRI), as contrast agents [56, 57] to detect bacterial urinary track infections [58], human immunodeficiency virus (HIV) [3, 59], and cancer cells [60].

Table 2. Specific possible biolayer as receptor molecules corresponding to structural integrity and output signal for molecular assemblages in biosensor applications

Biolayer type	Essential for structural integrity	Typical output signal	Complexity hierarchy
Ionophore (e.g., natural: gramicidin for K^+; synthetic: quaternary ammonium cationic surfactants for Cl^-, F^-, CN^-, SCN^-, etc)	Adequate retention	Electromotive force (EMF)/absorbance change (chromionophore)	↓ Increases ↓
Antibody	pH stability	Antigen uptake mass change	
Enzyme	pH/electrolyte stability	Reaction product	
Biomembrane (e.g., receptor)	Mechanic protection	Released contents	
Cell organelle (e.g., Mitochondrion)	Osmotic/pH stability	Product of electron chain	
Whole-cells or tissues (e.g., virus and bacteria)	Nutrient/oxygen supply	Metabolic end product	
Central nervous, renal, hormonal and cardiovascular systems	Nurotransmeter	Voltammetric response	
End of organ (e.g., Olfactory)	Intact tissue architecture	Action potential	

Table 3. Different biosensors corresponding to sensing biorecognition materials, immobilization methods (on transducer surface), sensing elements used, and transducing processes

Biorecognition material	Immobilization method (on transducer surface)	Sensing element	Transducing Process
Immunochemical, enzymatic, nonenzymatic;	Physical adsorption at solid surface, covalent binding to a surface;	Electrical potential, current, conductance, and impedance;	*Electrochemical (catalytic):* Potentiometric, voltametric, aperometric, conductometric, impedimetric, capacitive;
Nucleic acids (DNA, RNA);	Molecular crosslinking, entrapment within a membrane, surfactant matrix, polymer or microcapsule;	Intensity and phase of EM radiation;	*Optical affinity/Light scattering:* Light absorption, fluorescence/ phosphorescence, bio-chemiluscence, reflectance, Raman scattering, refractive index, ring resonator or ellipsometric, internal reflectance, surface plasmon resonance, photonic crystal, optical fibers, interferometer;
Antibody/antigen, biomimetic materials;	Sol-gel entrapment;	Viscosity;	*Acoustic/Mechanical:* Acoustic plate mode (piezoelectric), surface wave sensor, flexural wave sensor, love wave sensor, magnetic acoustic resonator;
Microorganism;	Langmuir-Boltz (LB) deposition;	Mass;	*Mass sensitive/cantilever biosensor:* Piezoelectric;
Whole-cells (virus, bacteria)	Self-assembled biomembrane	Temperature; Paramagnetism	*Thermal sensors*; *Magnetic*

3. CRYSTAL STRUCTURE DEVELOPMENT AND MECHANISMS OF PIEZOELECTRICITY

3.1. Crystal structure

The piezoelectric material has ability to produce electricity under pressure (i.e., called direct piezoelectric effect or piezoelectric effect) and vice versa (i.e., called inverse piezoelectric effect). The piezoelectric sensor can be operated in three modes such as transverse, longitudinal, and shear depending on how a piezoelectric material is cut (e.g., A-cut, B-cut, etc.). The most common type unit cell structure of piezoelectric material is perovskite, general formula 'ABX$_3$'. Where, the A-site cations are typically larger than the B-site cations and almost similar in size to the X-site anions, i.e., oxygen (O). A general unit cell structure of piezoelectric material is depicted in Figure 2a. The 'A' and 'B' may be three different combinations of metallic atoms/ions at different lattice position in a unit cell [61]. First, 'A' and 'B' may be both trivalent (e.g., $LaAlO_3$). Second, 'A' may be divalent (Ca, Sr, Ba, Cd, and Pb) and 'B' may be quadrivalent (Ti, Zr, Th, Zr, Hf, Sn, and Ge) (e.g., $CaTiO_3$). Third, 'A' may be univalent and'B' may be pentavalent (e.g., $NaWO_3$). In perovskite compound, A-site cations are surrounded by twelve anions in cubo-octahedral coordination (i.e., the atoms are surrounded by six anions in octahedral coordination), and B-site cations are octahedrally coordinated by anions, and the X-site anions are coordinated by two B-site cations and four A-site cations; these octahedra share apices [62, 63].

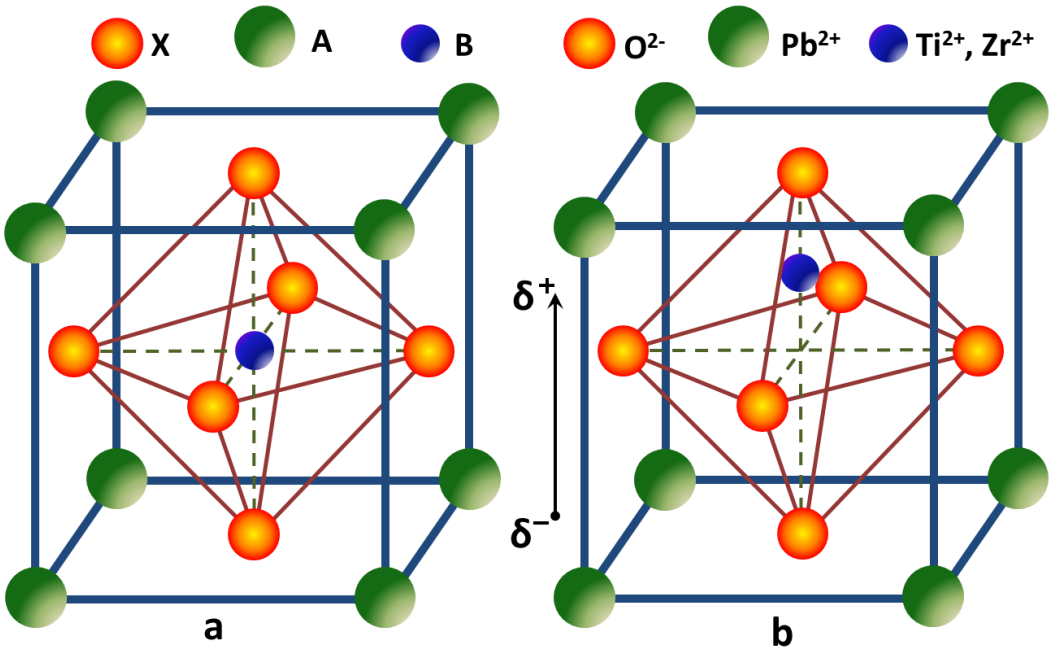

Figure 2. (**a**) Structure of piezoelectric material [63] and (**b**) Structure of PZT under an electric field [64].

In this context, $PbTiO_3$ (PT) is one of the simplest perovskite piezoelectric materials. The relaxor-PT ceramic-ceramic composites (e.g., $PbZn_{1/3}Nb_{2/3}O_3$-$PbTiO_3$ (PZN-PT), $PbMg_{1/3}Nb_{2/3}O_3$-

$PbTiO_3$ (PMN-PT)) have shown very high-electromechanical coupling properties and low-dielectric loss, that can be used as acoustic sensors or transducers in ultrasound and acoustic measurements for advanced biomedical applications [64, 65]. Direct piezoelectricity of polar semiconductors such as aluminium nitride (AlN) and zinc oxide (ZnO), and ferroelectric PZT ($Pb(Zr,Ti)O_3$) films has been widely studied [66-69]. PZT is often used in a specific composition, sometimes with additives, in order to achieve a particular crystal structure and a desired piezoelectric response. An equilibrium structure of PZT is similar to the Figure 2a, where $A=Pb^{2+}$, $B=Ti^{2+}$ and Zr^{2+}, and $X=O^{2-}$. The radii of the atoms and their bonding affinity lead to a lattice as rigid, while affording some freedom to the positive ions, in the center of the unit cell (i.e., meeting point of solid diagonals), to move within the structure under external force such as force, pressure, stress, strain, heating, and electric or magnetic field. A unit cell structure of PZT under influence of an external electric field is depicted in Figure 2b. This helps to get polarization in PZT crystal under external effect by moving of B-type atom(s) from the original center position. The movement of B-type atom(s) generates a charge deviation, which provides electricity in the piezoelectric material. The material expands slightly along the axis of the electric field and contracts a little in the perpendicular direction. There are so many developments in phase diagram of PZT crystals. A generally accepted phase diagram of PZT says that the ferroelectric compositions with rhombohedral and tetragonal symmetry on the two sides of the morphotropic phase boundary (MPB) the polar axis are <111> and <001>, respectively, as depicted in Figure 3 [70, 71]. The MPB which separates rhombohedral Zr-rich from tetragonal Ti-rich PZT is very narrow composition range i.e., called morphotropic phase composition (MPC). This phase boundary is not well defined owing to its associated coexistent phase region whose width depends on the compositional homogeneity and on the sample processing conditions [70]. Under loading condition the ferroelectric rhombohedral phase is transformed into ferroelectric tetragonal phase, which is mainly responsible for change in charges or polarizations at piezoelectric crystal surfaces.

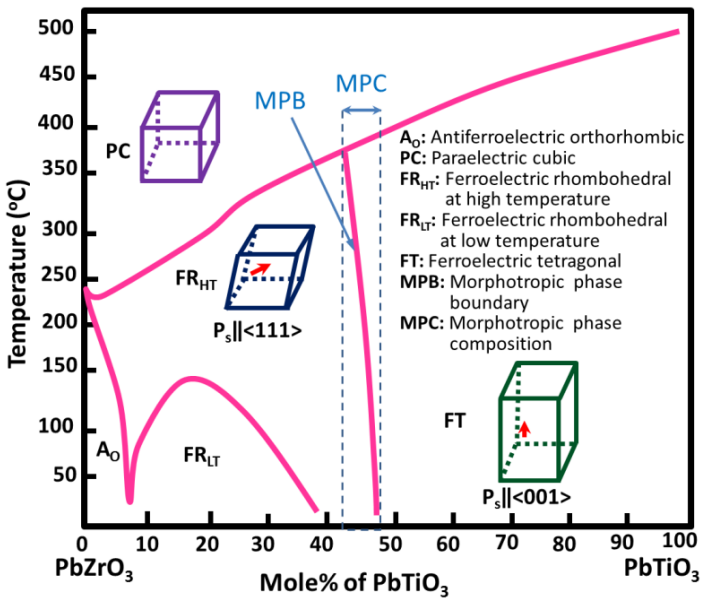

Figure 3. Phase diagram for PZT, with relevant regions labeled [70].

Recently, lead-free ferroelectric compound such as $BiFeO_3$ shows potential properties for piezoelectric devices because of its spontaneous polarization as high as $100\mu C/cm^2$ and high Curie temperature (T_C=850˚C i.e., at which spontaneous polarization is lost on heating) [72]. $BiFeO_3$ is a rhombohedral perovskite with space group R3c [73]. It has shown many advantages in biosensor device applications [74]. Thinfilms of $BiFeO_3$ are reported to have lower permittivities than Pb-based ferroelectric materials [75, 76]. Other lead-free piezoelectric ceramics materials such as $BaTiO_3$ (BT), $KNbO_3$ (KN), etc also show a large piezoelectricity and high T_C.

3.2. Synthesis techniques of piezoelectric materials

Several natural materials such tendon, bone, dentine enamel, DNA, baleen whale, sugar cane, quartz crystal, topaz, rochelle salt and so on have shown piezoelectric properties [77]. Some of these materials are shown in Figure 4. Since synthetic materials have shown better smart properties as sensors and actuators, several synthesis methods have been developed for piezoelectric crystals. The commonly used synthesis techniques of piezoelectric materials are illustrated in Table 4.

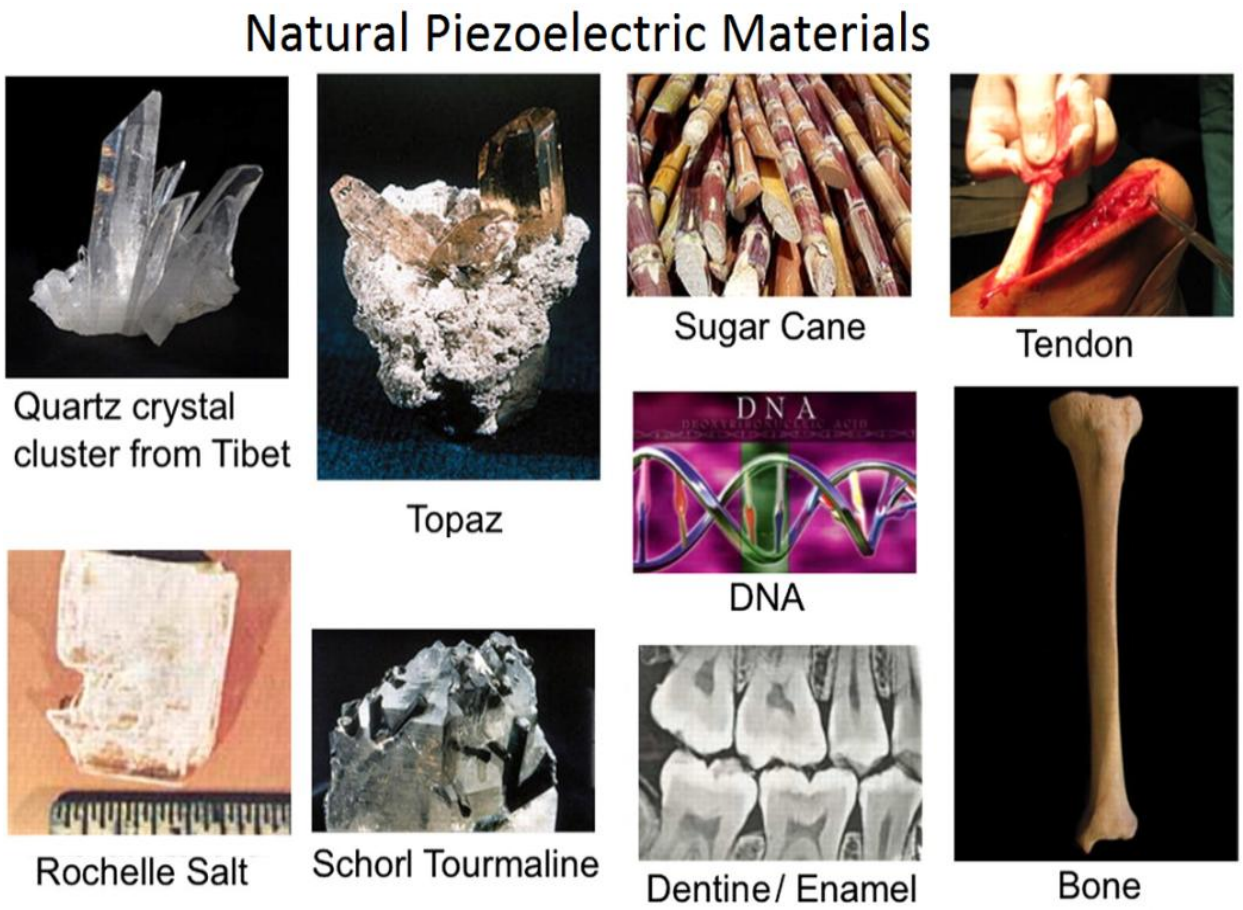

Figure 4. Natural piezoelectric materials that produce electricity under pressure and vice versa; reproduced from [77].

Table 4. Synthesis techniques of piezoelectric materials

Synthesis technique	Piezoelectric materials	References
Hydrothermal	quartz, PZT	[78, 79]
Sol gel	PZT, $BiFeO_3$	[80, 81]
Pulsed laser deposition	TiN/$Pb(Zr_xTi_{1-x})O_3$, PZT	[82, 83]
Solid state reaction	$BiFeO_3$, PZT	[84, 85]
Co-precipitation	$BiFeO_3$	[86]
Ferrioxalate precursor	$BiFeO_3$	[87]
Microemulsion	$BiFeO_3$	[88]

The piezoelectric materials have plenty of applications such as optics and photonics [89], precision mechanics [90], biomedical and medicine [91], vibration control [92], measuring technologies [93-95], microelectronics [96], and so on. Recently, PZT and their polymeric composites have also shown plenty applications [91, 96, 97].

3.3. Mechanism

In direct piezoelectric effect, mechanical stress arising on the surface of piezoelectric crystal as a result of external force acting on the piezoelectric body induces positive or negative displacement in the lattice elements which manifest themselves in dipole moments. This is typically shown as a vector extending from the negative charge to the positive charge. When a piezoelectric crystal is loaded by mechanical force, the crystal is being compressed, twisted or pulled and the molecular dipole moments are re-oriented themselves. The resulted electric field develops an electric potential on the insulated electrodes. This is occurred when the tetrahedron of piezoelectric crystal is pressurized with an applied force, the cation charges move towards the centre of the anion charges. In inverse piezoelectric effect, the amount of deformation is a function of the polarity of the voltage applied and the direction of the polarization vector. An applied AC voltage can generate a cyclical change in the geometry (e.g., increase or decrease in the diameter of a disk). When an electric field is applied across a piezoelectric medium, there is a slight change in the shape of the dipoles causing a very small but significant change in the material dimensions. In this instance, if the crystal is fixed (i.e., deformation is constrained), a mechanical stress or force is evolved. Using this piezoelectric principle, the piezoelectric sensor devices measure acceleration, pressure, load, strain or force and convert them to an electrical signal. This converse effect enables a piezoelectric material to produce an ultrasound pulse. The piezoelements are mostly suitable for the detection of dynamic processes.

Piezoelectric crystals are most important material for sensors and actuators, owing to its remarkable piezoelectric performance. The characteristic of the piezoelectric effect is very similar to the effects of electric dipole moment in a solid. The dipole density or polarization of a crystal can be calculated by integrating the dipole moments per volume of the crystallographic unit cell [98]. Resonance properties of the poled piezoelectric specimens can be measured using an HP 4194A Impedance Analyzer [99]. The efficiency of energy conversion, k^2, (where, k is effective electromechanical coupling coefficient of the piezoelectric material) of the radial test specimens can be

calculated using the resonance/antiresonance method expressed by a simplified relation as mentioned in Eq.(1) [100].

$$k = \sqrt{\frac{electrical\ energy\ output}{mechanichal\ energy\ input}} = \sqrt{\frac{mechanichal\ energy\ output}{electrical\ energy\ input}} = m\sqrt{\frac{E}{\varepsilon_0 \varepsilon_r}} \quad (1)$$

where, m is the piezoelectric 'motor' coefficient, defined as the rate of change of strain with field, E is the Young's modulus of the material, ε_0 is the permittivity of free space (i.e., ~ 8.85×10^{12} Fm^{-1}), and ε_r is the relative permittivity of the material. The piezoelectric coupling coefficient (k) also can be expressed as Eq.(2) [97].

$$k = \sqrt{\left(\frac{E}{\varepsilon}\right)} d \quad (2)$$

Where ε is dielectric constant and *d* is piezoelectric strain coefficient.

4. ADVANTAGES OF PIEZOELECTRIC BIOSENSORS OVER OTHERS

Several transducing processes, such as electrochemical, thermal, magnetic, electromagnetic, optical or light scattering, and piezoelectric, have been used in biosensor devices over the last few decades. In this regard, piezoelectric transduced biosensors have shown several potential advantages in biomedical applications. The piezoelectric crystal (PZC) becomes electrically polarized when it is subjected to a mechanical stress. Conversely, it experiences a strain in response to an applied electric field, proportional to the field strength [101]. An ideal piezoelectric substrate material for a biosensor has to be nontoxic with outstanding mechanical, thermal, and semiconducting properties. Several kinds of piezoelectric materials that have been used as transducing or sensing elements, so far, are ceramics (e.g., lead zirconate titanate or PZT ($PbZr_{0.52}Ti_{0.48}O_3$), quartz (SiO_2), AT-quartz cut, BT-quartz cut, lithium niobiate ($LiNbO_3$), and lithium tantalate ($LiTaO_3$)) [102, 103], polymers (e.g., PVDF, etc), rubbers (e.g., polydimethylsiloxane (PDMS) stamps or soluble glues) [101], and composites (e.g., PZT/PVDF, PBLG/PMMA, etc) [12]. In this context, the ceramic piezoelectric materials have shown excellent chemical stability and can perform at elevated temperature. Quartz crystal shows a strong piezoelectric effect perpendicularly to its prism axis. The electrical polarization is generated by applied pressure on a quartz crystal along the pressure direction. Conversely, a mechanical deformation of the crystal can be generated by applied electrical field. The quartz crystal is trigonal crystallized silica (SiO_2). A single crystal perovskite structured material, such as PZT, is an extremely efficient class of piezoelectric energy conversion materials. The energy conversion efficiency from mechanical to electrical form can be more than 80% in a PZC device, when it is operated nearly at resonance [103]. The PZC exhibits attractive electro-acoustic property spectra, and strong piezoelectric properties with applied stress and temperature. On the other hand, piezo-films are made of engineering polymers or composites. The composite piezo-films are more flexible, lightweight, and tough. It has a wide variety of thicknesses and a large working area compare to ceramics. A major advantage of the piezo-films over piezo-ceramic crystals is low acoustic impedance, which is closer to water, human tissues, and other organic materials. This advantage offers a real-time output, practical simplicity, and cost

effectiveness. Biomolecules, such as enzymes, lipids, antibodies, and antigens, have been used as specific coatings on different substrates for detection. Several methods of protein coating have been explored for numerous applications such as DNA hybridization, microbial assays, microgravimetric immunoassays, enzyme detections, and gas phase biosensors. In this context, the piezoelectric immunochemical sensor is most convenient to use and very promising to recognize the various biomolecules [104]. A growth of piezoelectric technology is directly related to a set of inherent advantages. Whilst the piezoelectric sensors react to compression under electromechanical systems, the sensing elements show almost zero deflection. As a result, the piezoelectric sensors exhibit an extremely high natural frequency and excellent linearity over a wide amplitudes range. Additionally, the piezoelectric technology is insensitive to electromagnetic field as well as radiation and enables to measure under harsh conditions. Some piezoelectric crystals (e.g., tourmaline) can also show electrical signals by changing their phase. One of the great advantages of the piezoelectric biosensors over other sensors is that it transduces a very high direct-current (DC) output impedance, which can further amplify the recorded signals.

5. DEVELOPMENT OF ADVANCED PIEZOELECTRIC BIOSENSORS

5.1. Characteristic features

The characteristic features of piezoelectric biosensors are involved with the change in resonant frequency. The resonant frequency change results from the mass change associated with binding between an analyte and its complementary anti-analytes immobilized onto receptor electrode surface.

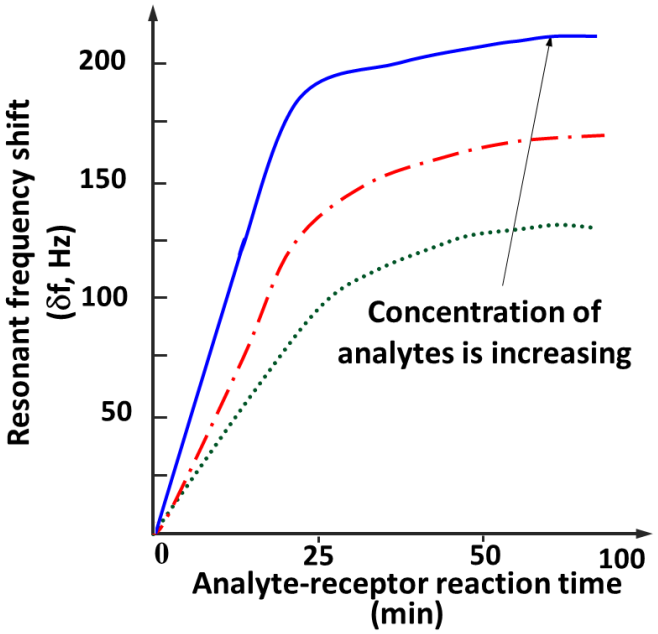

Figure 5. Characteristic behaviour of resonant frequency shift (δf) vs analyte-receptor reaction time with different concentrations (all the units are taken as arbitrary) [107].

After the first publishing of a novel discovery by Sauerbrey in 1959 [105], it has been established that the resonant frequency shift of a PZC in a fluid medium can be modulated with change in mass, coating thickness, density, viscosity, temperature, conductivity, permittivity, and so many physicochemical parameters of the fluid [106]. A common relationship between the resonant frequency shift (□f) and analyte-receptor reaction time with various concentrations of analytes is depicted in Figure 5. The Figure 5 reveals that the □f initially increases sharply with time, but after a saturation time, the □f becomes constant or stable and independent of reaction time. This saturation time possibly indicates the completion of the reaction in a particular molecular system [107]. This behaviour is applicable for any concentration of an analyte system. However, the □f is always greater for higher concentration of a particular analyte system.

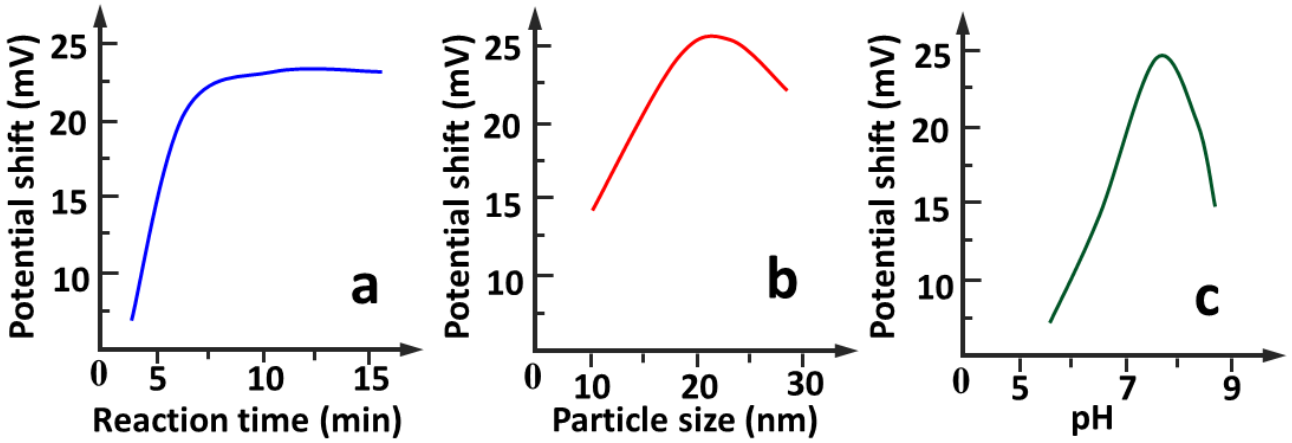

Figure 6. Effect of **(a)** reaction time, **(b)** size of gold nanoparticle and **(c)** pH of the solution on the potential shift of an immunobiosensor at a particular concentration of analyte (all the units are taken as arbitrary) [13].

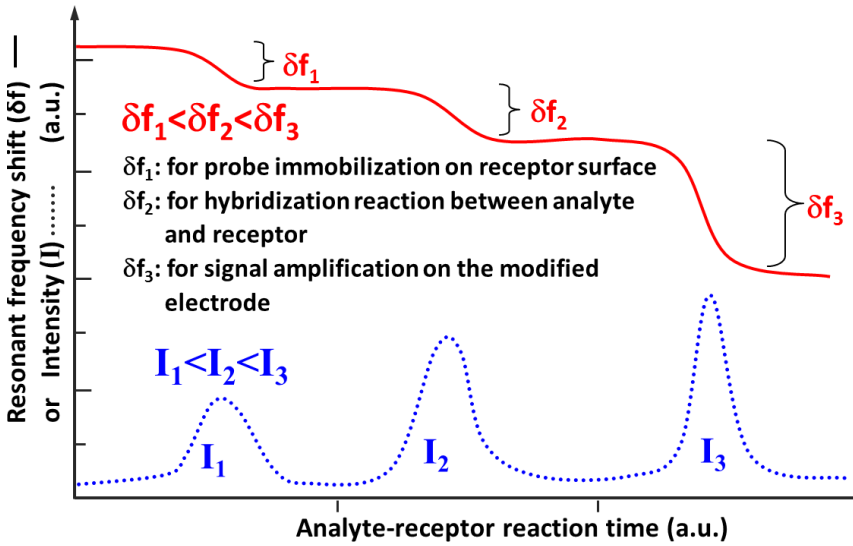

Figure 7. A general time-dependent frequency shift and signal intensity of a QCM sensor for: addition of probe to self-assembly immobilize on the surface of the QCM sensor, a complementary target with receptor material or biomolecule, and additional treatment of the hybridized QCM with modified electrodes [9].

Similarly, for a particular concentration of an analyte system, the potential shift also behaves in a manner as similar to resonant frequency (Figure 6a). However, the potential shift, after reaching a maximum value, decreases with the pH of the solution (Figure 6b) and the particle size (Figure 6c) of the receptor-electrode nanomaterial [13]. In quartz crystal microbalance (QCM) sensors (Figure 7), both frequency shift and signal intensity gradually increase with the addition of (i) the probe to a self-assembled immobilized QCM surface (see Δf_1 and I_1), (ii) the complementary target with receptor material or biomolecule (see Δf_2 and I_2), and (iii) a treatment between the hybridized QCM and modified electrodes (see Δf_3 and I_3) [9].

The resonant frequency of an oscillating PZC affected by a change in mass at crystal surface has been applied to monitor the vapour deposited chromatographic gasses [37], enzyme [39], and protein [108]. At resonant frequency, the oscillation becomes maximal, even at a small periodic driving force, because the system stores vibrational energy. The Δf should be as high as possible to correspond to a minimum mass change (Δw) in a high performance piezoelectric biosensor device. The use of PZC as a mass sensitive sensor is based on the well-known Sauerbrey-equation [105] that displays a linear relationship between the Δw and Δf in Eq. (3):

$$\delta f = -\frac{2f_0}{A}\left[\frac{1}{\rho_Q \mu_Q}\right]^{\frac{1}{2}} \Delta w \qquad (3)$$

where, f_0 is the fundamental oscillation frequency of PZC in MHz, A is the total surface area of the quartz sensor electrode (cm^2), μ_Q is the shear modulus (i.e., 2.947×10^{11} $g/cm.s^2$) of quartz, and ρ_Q is the density (i.e., 2.648 g/cc) of quartz. The Δf (in Hz) corresponding to a Δw (in μg) of a quartz PZC biosensor depends on the simplified governing equation Eq. (3) and is expressed in Eq. (4) [108].

$$\delta f = -\frac{\Delta w}{w f_0} \qquad (4)$$

Where, w is the crystal mass (μg). In this context, Muramatsu *et al.* (1987) [108] showed that a PZC modified with immobilized protein-A coating can be effectively applied to determine the human immune globulin (IgG) protein with various IgG-subclass concentrations. It has been found that 1 ml of 10^{-6} mg/ml human IgG solution can give 8 Hz of Δf, and 1 ml of 10^{-5} mg/ml human IgG solution can give 33 and 22 Hz of Δf. The magnitude of each parameter may also be affected by the characteristics of each resonating crystal. In this context, Kanazawa and Gordon (1985) [109] had ascertained an equation (Eq. (5)) obtained from a physical model of shear waves in a quartz crystal and damped shear waves setup in a fluid during resonance.

$$\delta f = -f_0^{3/2}\left[\frac{\rho_L \eta_L}{\pi \rho_Q \mu_Q}\right]^{\frac{1}{2}} \qquad (5)$$

Where, η_L and ρ_L are the absolute viscosity and density of the fluid or liquid, respectively.

The thickness (t in cm) of a PZC can shift its resonant frequency as presented in equation Eq. (6) [110].

$$\delta f = -\frac{2f_0 \Delta w}{A t \rho_Q} \qquad (6)$$

The Sauerbrey-equation also can be derived in terms of stress, thickness, and radius. For a homogeneous membrane, which is perfectly clamped at the boundary, the resonant frequency (f_{ij}) can be expressed by equation Eq. (7) [111]:

$$f_{ij} = \frac{\alpha_{ij}}{2\pi R}\left[\frac{\tau}{\rho t}\right]^{\frac{1}{2}} \tag{7}$$

where, α_{ij} is a dimensionless parameter, i and j are integers, and R, τ, t, and ρ are the radius, stress, thickness, and density of the membrane, respectively.

For an acoustic biosensor, when the mass load (ω) is uniformly distributed on the surface and much smaller than the overall mass of the vibrating system (m), the mass sensitivity (S_ω) can be expressed as equation Eq. (8) [111]:

$$S_\omega = \frac{f_{ij}}{2m} = \frac{\frac{\alpha_{ij}}{2\pi R}\left[\frac{\tau}{\rho t}\right]^{\frac{1}{2}}}{2\pi R^2 \rho t} = \frac{\alpha_{ij}}{4\pi^2 R^3}\left[\frac{\tau}{\rho^3 t^3}\right]^{\frac{1}{2}} \tag{8}$$

For a multilayer membrane, the density (ρ) from Eq. (7) and Eq. (8) can be represented in terms of effective density (ρ_e) and total thickness (Σt_i), as shown in Eq. (9).

$$\rho_e = \sum \frac{\rho_i t_i}{\sum t_i} \tag{9}$$

Where, ρ_i and t_i are the density and thickness of each membrane layer.

Depending on the Eq. (7), the resonant frequency of a membrane can be effectively controlled by the mechanical parameters (e.g., thinfilm stress (τ)) of membrane rather than the material parameters (e.g., Young's modulus that is significantly different for membrane and plate). Therefore, the τ of a single layer membrane for before and after thinfilm coating can be calculated by Eq. (10) and Eq. (11), respectively.

$$\tau = \frac{4\pi^2 R^2 t \rho_e f_{ij}^2}{\alpha_{ij}^2} \tag{10}$$

$$\tau^c = \frac{4\pi^2 R^2}{\alpha_{ij}^2}\left[t^c \rho_e^c f_{ij}^{c2} - t\rho_e f_{ij}^2\right] \tag{11}$$

Where, τ^c, t^c, ρ^c_e, and f^{c2}_{ij} are the stress, thickness, effective density, and frequency, respectively of the membrane after coating.

5.2. Materials development for the detecting part of biosensors so far

Since the sensing property is a basic requirement for a detecting material, it is one of the major vital steps in the development of biosensors. In this instance, mostly, metallic nanoparticles or nanowires are generally used as electronic conductive components, and oxide nanoparticles are often applied to immobilize the biomolecules. On the other hand, semiconductor nanoparticles are often used as labels or tracers [112].

Table 5. Applications, advantages, and disadvantages of different detecting materials system for advanced biosensors

Detecting material	Application	Advantage	Disadvantage	Reference
Silicon or quartz [e.g., silicon (Si) crystal and silicon oxide (SiO_2)]	Detection of mycobacterium tuberculosis	Low cost, mature processing techniques	Limits in operating frequency range	[116]
Organic semiconductors [e.g., cadmium sulphide (CdS), cadmium selenide (CdSe), cadmium telluride (CdTe), indium phosphide (InP), indium arsenide (InAs), lead selenide (PbSe), etc.]	Optoelectronics, deoxyribonucleic acid (DNA) printing	Ease of application (Inkjet printing, spin casting), suitability for flexible substrates, suitability for optoelectronics	Low carrier mobility, not amenable to standard process flows	[117]
Compound semiconductors [e.g., gallium arsenide (GaAs), gallium nitride (GaN), doped gallium arsenide antimonide (GaAsSb), etc]	Optoelectronics	High carrier mobility, high frequency operation, suitability for optoelectronics, capability of band-gap engineering and epitaxially grown layers	Costly	[118]
Nanomaterials [e.g., silver (Ag), platinum (Pt), palladium (Pd), GNPs, Au/HAp hybrid, Au/HAp/Chitosan nanocomposites, CNTs, magnetic nanoparticles, and quantum dots (CDs)]	Tumour biomarkers as alpha-fetoprotein, efficiency of gene delivery system	Novel physical, chemical, mechanical, magnetic and optical properties, and significantly enhancement of the sensitivity and specific detection ability	Unproven safety profile, not amenable to standard process flows	[4, 13, 27, 51, 55, 113-115, 119-122]
Hydroxyapatite (HAp) nanoparticles	Nucleic acid or DNA sensing	HAp excellent ability to absorb the functional biomolecules, including protein, DNA, etc; high variation in electronic state of receptor and transducer biomolecules	Low flexibility	[123]
HAp/nafion composite	Glucose biosensing, immobilization of enzymes	Enhanced stability and sensitivity of the biosensor, better flexibility	Low lifetime	[124]
Horseradish peroxidase (HRP) on silica–HAp hybrid film-modified glassy carbon electrode (GCE)	For H_2O_2 biosensors by direct electron transfer of immobilized HRP on silica–HAp hybridized GCE	Fast electron transfer process, excellent electrocatalytic response to the reduction of H_2O_2 without the aid of an electron mediator, high sensitivity to H_2O_2 with low detection limit, good reproducibility, HAp provides good microenvironment for the immobilization of protein	Low flexibility	[125]
HAp/poly(etheretherketone) (PEEK), nanoHAp/functional PEEK/carbon nanofibers (CNF) nanocomposites	Can be used for protein sensor	Would have high mechanical strength and flexible, enhanced stability and sensitivity of the biosensor, long life, cheapest	Low electrical conductivity	[126-128]

Recently, several kinds of nanomaterial have been used as detecting materials in advanced biosensors, owing to their unique physical, chemical, mechanical, magnetic, and optical properties. The nanomaterials also significantly enhance the sensitivity as well as molecular specificity [27] of

biosensors. These nanomaterials, such as quantum dots [51, 55, 113], magnetic nanoparticles [4], GNPs [114], and CNTs [115] have been used for these purposes. The important advantages and disadvantages of different detecting materials, commonly used in advanced biosensors, are illustrated in Table 5.

5.3. Typical immobilizations by surface modification for advanced applications

To improve the sensitivity of PZC biosensors, several methods, including optimizations of probe immobilization [129, 130] and various signal amplification strategies such as non-specific amplifiers of anti-dsDNA antibodies [131], enzymes, liposomes [132], and nanoparticles [133] have been developed.

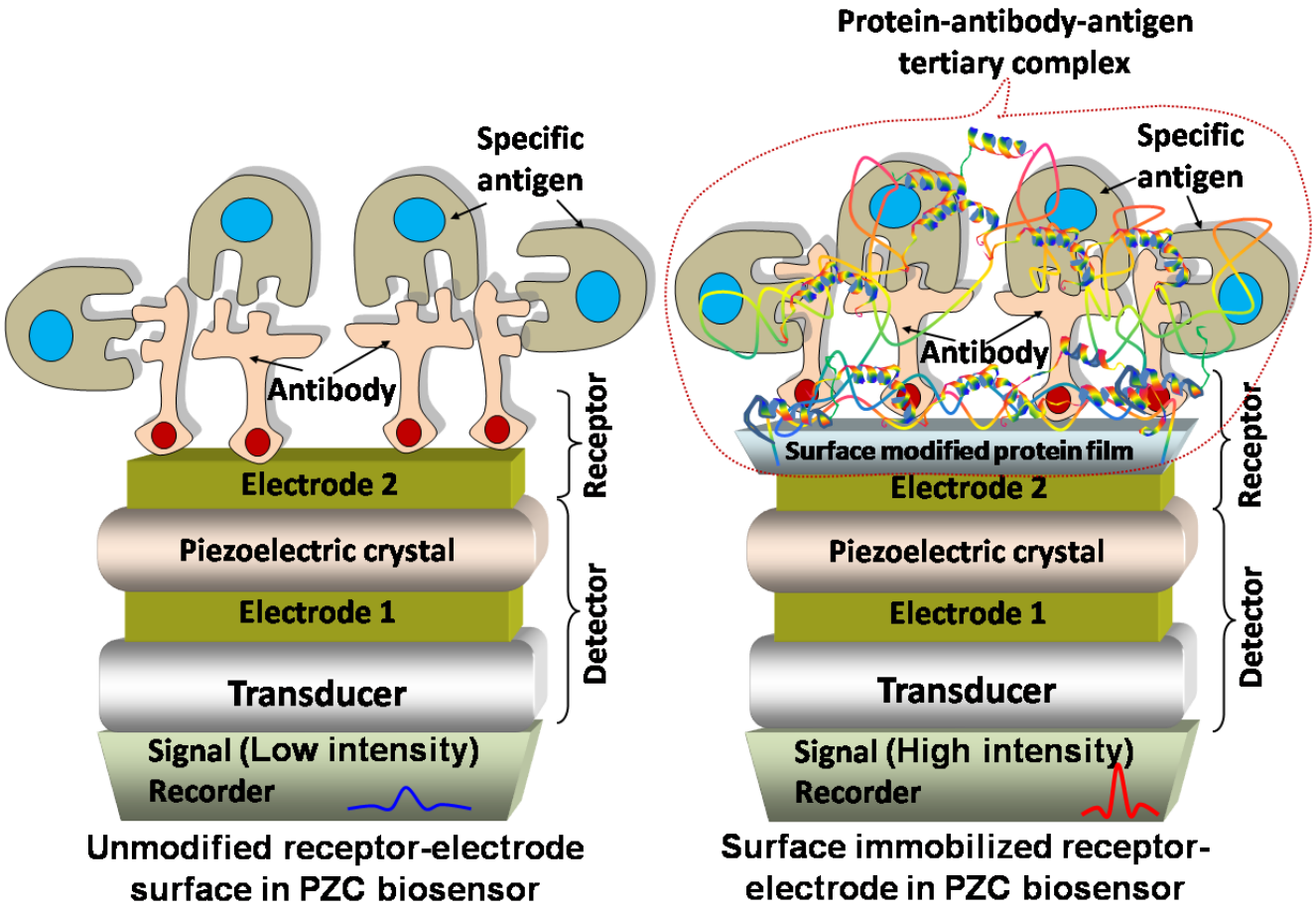

Figure 8. Typical advantage (i.e., high intense signal) of surface modified (right) piezoelectric biosensor over unmodified (left).

One of the crucial steps in the development of biosensors is immobilization of biological components at the electrode-surface of receptor. The most generally employed methods are physical adsorption at a solid surface [134], cross-linking between molecules [135], covalent binding to a surface [135], entrapment within a membrane [136], surfactant [137], and polymer or microcapsule

[138]. The other potential immobilization methods are sol-gel entrapment [139], Langmuir–Blodgett (LB) deposition [140], electropolymerization [141], self-assembled biomembranes [142], and bulk modification [143]. A typical advantage of surface modified piezoelectric biosensors over unmodified piezoelectric biosensors is depicted in Figure 8. The surface modified electrode coated with a biomolecule (e.g., protein attached with antibody) forms a tertiary protein-antibody-antigen complex after reacting to a complementary analyte structure (e.g., antigen) of the employed antibody. The functionalized receptor behaves like a key to its complementary analyte, which seems to be locked, during immobilization. This surface modification of the receptor electrode has potential advantages over bare electrodes in terms of accumulating or detecting higher amounts of analytes, resulting in an intense signal (see Figure 8).

Several attempts have been made to immobilize the analytes onto the bioreceptor by many chemical reactions in order to improve the sensitivity of biosensors. This is usually done by immobilization of bioreceptor materials or species onto the sensor surface. After a first use of this technique by Sauerbrey in 1959 [105], various kinds of inorganic and organic coatings have been used in the PZC biosensors. Numerous surface modification methods using different coating materials (viz., silane reagents, surface modified with YWG-$C_{18}H_{37}$ ligand, modified silica/HRP–HAp/GCE electrode, CS/MWCNTs/Au electrode, ZnO piezoelectric micromechanical membrane, etc) have been attempted to achieve a covalent attachment of modifier molecules or ions to the crystal surfaces. In the silane reagent method, the substituents such as alkoxy, amino, and chloro groups with hydroxyl group create a reactive surface via chemical reaction on the quartz substrate. On the other hand, the antibody-modified QCM surfaces are very attractive owing to their sensitivity, specificity, stability, and simplicity. Le *et al.* (1995) [107], had first modified the AT-cut piezoelectric crystal surface using YWG-$C_{18}H_{37}$ ligand, which is usually used as a protein purification ligand in chromatography. The quantity of immobilizing effect can be calculated by percentage of immobilized molecule from the equation Eq. (12) [144].

$$immobilized\ molecule = -\frac{w_{used} - w_{unbound}}{w_{used}} \times 100\% \quad (12)$$

Where, w_{used} is the amount of biomolecules used or attached to the crystal surface (μg) and $w_{unbound}$ is amount of unbonded biomolecules (μg).

A potential immobilization method for advanced biosensor is concisely generalized in the following steps:

(i) Selection: selection of suitable and cost effective PZC with compatible resonant frequency related to the application is the first major step of a surface immobilization.

(ii) Cleaning and drying: cleaning of the PZC is done with a suitable solution(s) for certain a time, and subsequently, the crystal is dried.

(iii) Deposition of thinfilm electrode: a highly conductive metallic thinfilm electrode is deposited as a receptor on the top and bottom faces of the PZC using several different techniques.

(iv) Surface modification: the relevant electrode surfaces are oxidized and/or activated with different selected reagents maintaining proper reaction conditions.

(v) Removing of unwanted material: the unwanted materials from the surface modified electrode are washed out after properly drying.

(vi) Immobilization with biomolecule: the activated or modified electrode-surface is chemically bonded with selected biomolecules. The selection of biomolecule highly depends on the target analyte biomolecules that would be used during applications.

(vii) Flocking: the untreated residual groups are blocked by an appropriate solute.

(viii) Cell contact: the receptor surface is ready to expose for specific cell contact.

The applied immobilization techniques, including selection of PZC and electrode materials, cleaning and drying process, coating or thinfilm techniques (TFT), proper solutions or media and its exposed time, and surface modifying agents and methods, may be different for different approaches. Thus, only important parts of some selected typical immobilization procedures using effective materials related to the purpose of this article are briefly specified.

5.3.1. Immobilization by □-APTES

In this method, an At-cut PZC with resonant frequency of few MHz (e.g., 9 MHz) is used as transducing element. The electrode materials, silver (Ag) and palladium (Pd) film, are deposited by vapour deposition method and electrochemical plating, respectively. The electrodes (i.e., conductive thinfilms) are anodically oxidized at constant current (e.g., 4 mA/cm^2) in sodium hydroxide (NaOH) solution (e.g., 0.5 M). The electrode is modified with (□-amino-propyl)triethoxysilane (□-APTES, 5% in acetone) at room temperature for about an hour. The modified electrode is dried in air and subsequently placed into glutaraldehyde solution (GA 5%, pH7) for few hours (e.g., 3 h). Protein-A (1 mg/ml, pH7, 0.05 M phosphate buffer) is then immobilized onto the electrode surface via an aldehyde for an hour. The remaining unreacted aldehyde is blocked with 0.1 M glycine (10 ml of stirred solution). Finally, the surface immobilized PZC is placed for cell contacts.

In this intense, Muramatsu et al. (1987) [108] had ascertained that the PZC-surface modified with an immobilized protein-A layer can be effectively employed to analyze the protein-protein (e.g., IgG and IgG-subclasses) interaction.

5.3.2. Immobilization by 2% YWG-$C_{18}H_{37}$ ligand

Prior to surface modification, AT-cut PZC is cleaned in a solution of 1.2 N NaOH and 1.2 N HCl for 30 min each followed by washing with distilled water and alcohol. After properly drying (nearly at 70°C), one side of the PZC is treated with a 1.5 ml solution, which contains 2% YWG-$C_{18}H_{37}$ ligand dissolved in a solution of ethanol (C_2H_5OH) and dichloromethane (CH_2Cl_2) (1:1), using a spinning device. The unbound materials are removed from the surface by methanol. The surface treated crystal is again modified with a 0.2 ml solution of ethylenediamine, alcohol, and 2.5% GA (2:3:2) by spinning followed by drying and washing with water. Subsequently, 10 µl of 5 mg/ml antibody solution is spread over the electrode surface. The unreacted aldehyde groups are flocked by immersing of crystal into a solution of 0.1 M glycine in 20 nM phosphorous buffer solution (PBS, pH 7) followed by air drying. Finally, the treated crystal is again washed with PBS and distilled water, successively, and dried properly.

In this instance, Le *et al.* (1995) [107] had investigated on goat-anti-human IgG to immobilize onto a surface modified PZC by measuring its resonant frequency shift owing to mass change for detecting the *S. aureus*. This kind of ligand shows iniquitous binding capacity and selectivity towards antibody. They proposed that it is cheap and has high sensitivity to detection, long term stability, and reusability.

5.3.3. Immobilization by carboxymethyl group

In this immobilization method, a gold coated quartz crystal is modified with thiol as well as carboxylated dextran to immobilize the streptavidin and biotinylated oligonucleotide. The freshly cleaned quartz crystal is immersed into a stable 1 mM ethanolic solution of 11-mercaptoundecanol at room temperature in dark (for ~ 2 days). The crystal is then washed with ethanol and milliQ water followed by sonication for 10 min in ethanol to remove the excess thiol. The ensued hydroxyl surface is reacted with a 600 mM solution of epichlorohydrin in a mixture of 400 mM NaOH and bis-2-methoxyethyl ether (diglyme) (1:1) for 4 h. The treated crystal is immersed in an alkaline dextran solution (at 0.3 g/ml into 100 mM NaOH) for about a day to get more hybridised structures. The surface is further functionalized with a carboxymethyl group in a solution of 1 M bromoacetic acid and 2 M NaOH overnight. The functionalized crystal is washed with milliQ water and placed in the photovoltaic cell (PVC). The functionalized crystal surface is then activated prior to covalent coupling with a 200 ml aqueous solution of 50 mM N-hydroxysuccinimide (NHS) and 200 mM 1-ethyl-3-(3-dimethylaminopropril) carbodiimide (EDAC). Then, the activated solution is substituted by a streptavidin solution (at 200 μg/ml into 10 mM acetate buffer of pH 5). After 20 min, the residual reacting sites are blocked with 200 ml ethanolamine hydrochloride (pH 8.6, 1 M water solution) solution. A biotinylated probe is added (i.e., 200 ml of a solution containing 8.5 μg/ml of probe in immobilisation buffer) after washing with the immobilized buffer. Finally, the immobilization of crystal is allowed to complete at room temperature for 20 min followed by hybridization.

This system can be applied to detect the other polymorphisms by selecting different probes that can be immobilized on the gold coated PZC [145]. The immobilized surface layer provides higher sensitivity in the detection of human DNA (i.e., extracted from blood) owing to formation of strong carboxylated dextran hybridised bond with streptavidin coated gold surface of the crystal.

5.3.4. Immobilization by protein-A

Here, a 10 ml aliquot of 10 mg/ml protein-A in phosphate buffer solution is spread on the surface of PZC, and subsequently, 10 ml of 0.1 M Na-acetate buffer (pH 4.69) is used to bring up the pH to 5.95. The properly cleaned PZC is then incubated at different optimum temperatures and times to get a high yield protein-A immobilized surface. Similarly, a few millilitres of antibody solution are spread over the crystal surface followed by incubation at a optimized temperature and time combination to obtain a high yield antibody immobilized surface.

In this instance, Babacan *et al.* (2000) [144] had statistically analyzed the effect of immobilized layers (i.e., immobilized antibodies with *Salmonella typhimurium*) at a certain frequency of the PZC to determine the sensitivity of the piezoelectric system. Their results indicate that the degree of antibody immobilization via protein-A adhered Au-surface (42.19±2.09%) is higher than the antibody immobilization through aldehyde groups of GA modified surface of a quartz crystal pre-coated with polyethylenimine (PEI) (31.69±0.3%).

5.3.5. Immobilization by CS/CNT

Since the mechanical and electrical properties of thin films are still under concern to the researchers, the surface modification by biocompatible nanocomposites might be a potential and novel approach for producing the advanced biosensors. Chitin has extensively been used in molecular separation, food packaging film, artificial skin, bone substitutes, and water treatment owing to its biocompatibility, biodegradability, multiple functional groups, and pH-dependent solubility in aqueous medium. It is a most abundant natural polymer on the earth. The coating of chitosan (CS) material is a deacetylated derivative of chitin. On the other hand, carbon nanotube (CNT) has very high surface area, extremely high mechanical strength, excellent electrical and thermal conductivity, and good biocompatibility. Thus, the CS/CNT nanocomposite is expected to improve the mechanical properties of thin films owing to the CNT. Prior to surface modification with CS/CNT nanocomposite, a QCM-Au electrode is oxidized with 1.0 mol/l HNO_3 for 10 sec followed by proper cleaning via stream and drying with air cleaner. The oxidized electrode may be scanned (at 0 and 1.5 V) against saturated calomel electrode in 0.20 mol/l perchloric acid ($HClO_4$) solution (at 50 mV/s) for sufficient cycles to obtain reproducible cyclic voltammograms. A 0.5% chitosan (CS) solution is then prepared by dissolving CS in 1% acetic acid (CH_3COOH) solution using magnetic stirring for about 2 h followed by filtration with 0.22 μm filter paper. A suitable amount of multi walled carbon nanotubes (MWCNTs) is then mixed with 1 ml of 0.5% CS solution and ultrasonicated over 15 min. Lastly, 10 μl of the CS/MWCNTs mixture is spread evenly with a syringe over the ultra-cleaned, dried (using high-purity nitrogen stream) and activated surface of QCM-Au electrode followed by drying finally at 37°C for a day.

One of the best results ascertained by Jia *et al.* (2008) [5] is that the contact angle of CS/MWCNTs modified Au electrode (47°) is significantly lower compare to Au (64°) and CS (52°) electrodes. This result favours the hydrophilicity of the CS/MWCNTs film in microenvironment for living cells and also indicates more adhesion, proliferation, and retention of bioactivity. Therefore, longevity or life of the adhered cells is expected to be better for biocompatible CS/MWCNTs film than the CS film. It has also been confirmed by fluroscent microscopic cell viability assay of stained human breast cancer cells (MCF-7) cultured on the CS and the CS/MWCNTs modified QCM electrodes. The result of the CS/MWCNTs modified QCM electrode showed higher number of green hills made by newly grown living cells than that of CS modified electrode [5].

5.3.6. Immobilization by horseradish silica/peroxide/HAp on glassy carbon electrode

In this method, first, a homogeneous hydroxyapatite (HAp) sol is prepared from phosphoric acid (H_3PO_4) solution (0.01 M) and calcium hydroxide [$Ca(OH)_2$] by titration and then, ultrasonication. Silica sol is then prepared by sonication for several minutes using 600 µl ethanol, 50 µl tetraethoxysilane (TEOS), 10µl 5mM NaOH, and 60 µl H_2O. After that, a stock solution is prepared by adding of HRP (2.0 mg/ml) into HAp sol (10 mg/ml). In order to modify the electrode, a 8 µl horseradish peroxide (HRP)/HAp stock solution (i.e., 2.0 mg/ml HRP into 10 mg/ml HAp sol) is dripped and dispersed evenly on the cleaned (with alumina slurry on chamois leather) glassy carbon electrode (GCE) surface and air dried. Then, a 10 µl silica sol is dripped on the electrode and dried again in air. Finally, the modified silica/HRP–HAp/GCE electrode is cleaned and stored in pH 7.0-PBS at 4°C.

In this instance, HAp nanoparticle is used as a matrix in HRP-immobilization and the silica is used as a fixed reagent to enhance the stability of the sensor. This immobilized surface also exhibits excellent electrocatalytic response in reduction of hydrogen peroxide (H_2O_2), and improved stability and sensitivity [125].

5.3.7. Immobilization by thin film ZnO

The sensitivity of a sensor can be improved by thin film technique. A zinc oxide (ZnO) membrane fabricated by MEMS technology is used as piezoelectric material. An electrode composed of Ti/Pt (size: 50 nm Ti and 100 nm Pt) is deposited on (100) crystal plane of a 4 inch silicon wafer with 1 µm thermally oxidized silicon (SiO_2) by a DC sputtering. Then, piezoelectric ZnO film of thickness 1.5 µm is deposited by magnetron sputtering. After that, a layer of metallic tope (50 nm Cr/100 nm Au) is deposited by magnetron sputtering; subsequently, it is patterned into round solid electrodes by lift-off method. Finally, the membranes are released by deep reactive ion etching (DRIE) from the backside of the wafer using the Bosch process [111].

The sensitivity of the thinfilm, ZnO membrane, for biosensor application can be significantly improved by reducing the size of the membrane or working at higher resonance mode [111].

5.3.8. Immobilization by cholesterol oxidase (ChOx) and MWCNTs hybrid composite

Immobilization of glassy carbon electrode (GCE) can also be employed by ChOx/MWCNTs hybrid composite. Prior to surface modification, a properly cleaned and dried GCE electrode is dipped into a sonicated solution of MWCNT in PBS and dried at room temperature. Again, it is dipped in a mixing solution of PBS (0.1 M), N-ethyl-N'-(3-dimethylaminopropyl) carbodiimide (EDC, 0.4 M), and N-hydroxysuccinimide (NHS, 0.1 M), and dried properly. This surface activated electrode is further functionalized with ChOx by immersing in a fresh phosphate solution containing 1 mg/mL ChOx. This surface immobilized electrode is rinsed with supporting electrolyte to be used as cholesterol biosensor. The by-product of this cholesterol oxidation reaction is H_2O_2, which can be further detected by changing in electroreduction current via ChOx/MWCNTs/GCE electrode. A

schematic of this reaction is illustrated in Figure 9 [146]. The reaction is stable, pH-dependent, and electroactive as produced on electrode surface. In this instance, the role of MWCNTs is not only to enhance the surface coverage but also to enhance the electrocatalytic activity to H_2O_2.The average surface-coverage of ChOx/MWCNTs/GCE electrode estimated by Yang *et al.*, (2011) [146] is about 1.86×10^{-11} mol/cm^2 that is higher than both of MWCNTs (1.58×10^{-11} mol/cm^2) and ChOx (3.53×10^{-11} mol/cm^2) modified electrodes.

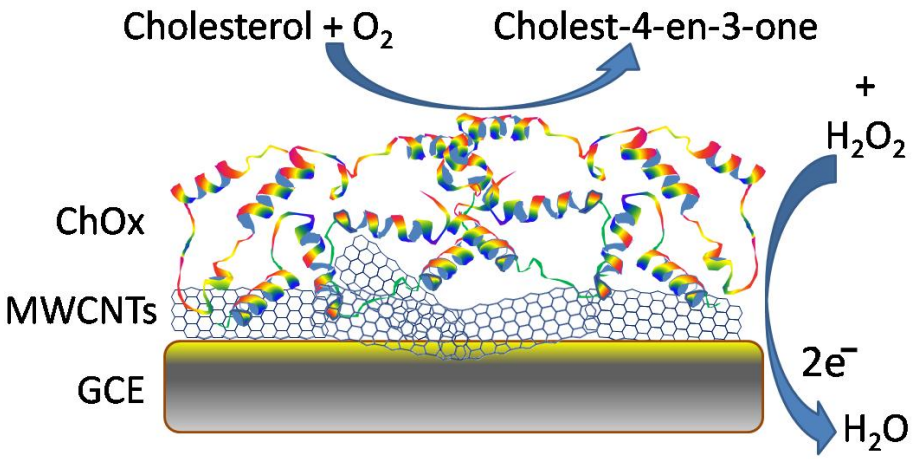

Figure 9. Electrocatalytic reaction of cholesterol by ChOx/MWCNTs modified electrodes [146].

6. MATERIALS FOR NEW GENERATION BIOSENSORS

The HAp nanoparticles with a high electrical conducting nanomaterial (e.g., Au, Ag, conducting polymers, etc) can be a potential candidate for detector part of the PZC biosensor. To improve the sensitivity of PZC in an advanced biosensor, surface modification of bioreceptor or electrode is one of the best steps. Greater surface area of the highly bioactive nanoHAp wires may give a better affinity towards the biomolecules, including proteins and cells. Nanowires of metal, alloys, conducting polymers, and CNTs will show maximum sensitivity in any biosensor owing to their high electron transport capability. The piezoelectric immunochemical sensor may be convenient to use promisingly. However, a thorough understanding of the different phenomena associated with crystal-frequency measurements linked to the reactions in a biological environment is still needed and deserves more careful study [104]. Presently, the fragile nature of ceramic piezoelectrics is being avoided by using organic piezoelectric materials. However, some drawbacks of organic piezoelectric biosensors need to be corrected. For example, the piezoelectric coefficient, d_{33}, for PVDF (i.e., -26 pm/V) polymer is an order of magnitude smaller than that of ceramic PZT (i.e., >250 pm/V); and PZT/PVDF composites show high performance but rapidly degrade in air [91].

Recently, the transducer properties play key role to design of diagnostic and therapeutic ultrasound systems. In this intense, multimaterial piezoelectric fibers have shown excellent properties as piezoelectric pressure transducers and it is depicted in Figure 10 [77, 147]. These multimaterial

fibers can act as ultrasound sensors as well as emitters and possess the potential for improving the quality of ultrasound imaging [77]. It could find a path in the next generation of ultrasound transducers and medical imaging. A structure of a multimaterial piezoelectric fibre is depicted in Figure 10a. The multimaterial fibers are consolidating a shell of poly(vinylidene difluoride-trifluoroethylene) (P(VDF-TrFE)), shells containing carbon-loadedpoly(carbonate) (CPC)/indium electrodes and poly(carbonate) (PC) cladding. The near-field pressure patterns of the acoustic emission at 1.3 MHz from a circular fiber, a triangular fiber and a rectangular fiber with cross-sectional dimensions about 2 mm are also shown in Figure 10b.

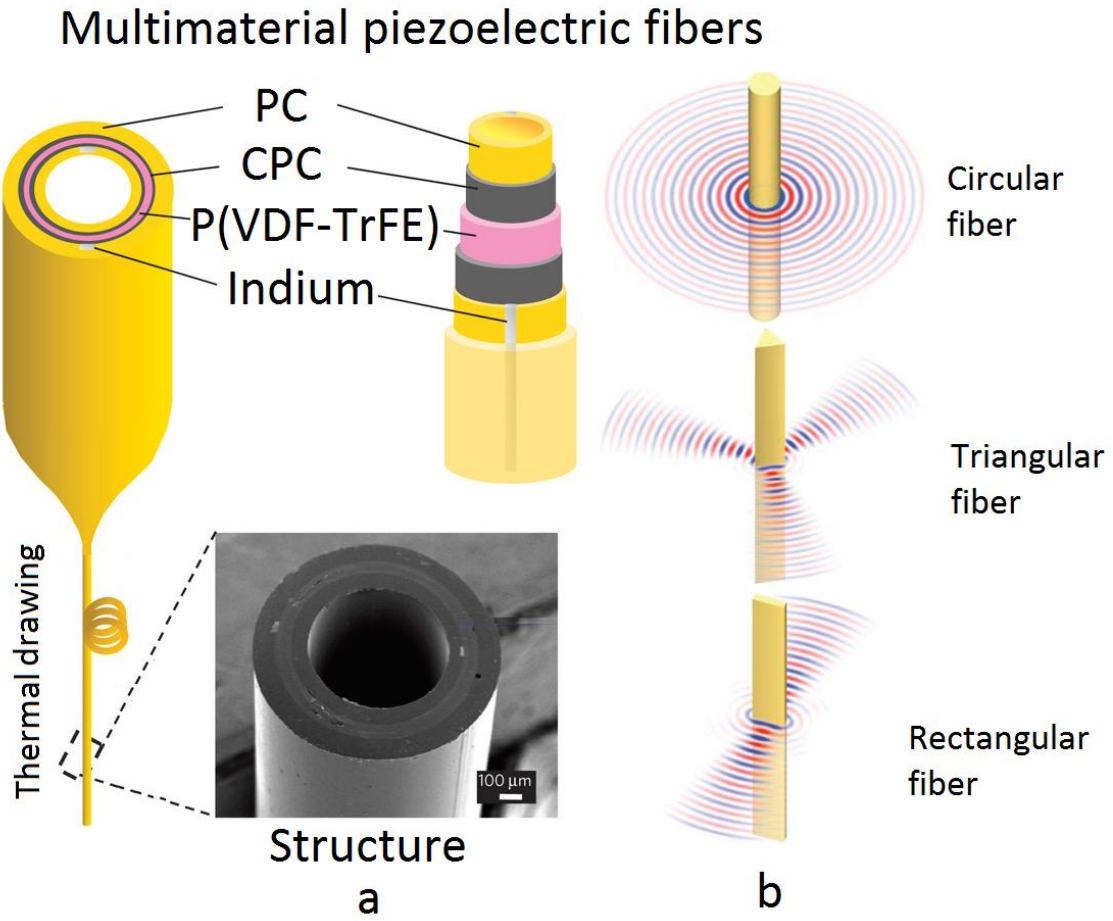

Figure 10. (**a**) A schematic of a cylindrical multimaterial piezoelectric fiber. The multimaterial fibers consolidating a shell of poly(vinylidene difluoride-trifluoroethylene) (P(VDF-TrFE)), shells containing carbon-loadedpoly(carbonate) (CPC)/indium electrodes and poly(carbonate) (PC) cladding. (**b**) Near-field pressure patterns of the acoustic emission from a circular fiber, a triangular fiber and a rectangular fiber with cross-sectional; (Reproduced with permission [147]).

7. CONCLUDING REMARKS

The PZC biosensor is one of the cheapest and simplest devices in this field. A high quality PZC biosensor can detect biomolecules up to nanogram levels of substances so far. From our peer review,

we conclude that the surface immobilized PZC would have the ability to detect biomolecular materials or species within a wide range of substances, possibly below nanogram level, even upto picogram, which is loaded onto the receptor-surface. Therefore, the functionalized materials having proper functional groups and the surface immobilization technique can play a vital role in significant improvement to cost and quality, including sensitivity, of the advanced biosensor devices. Recently, tissue engineering scaffolds are being used as a novel strategy for bone tissue repair and/or regeneration [148]. However, so far, no biosensor has been developed for the monitoring of hard tissues in orthopaedic applications since the monitoring of growth of neo-tissues to the scaffolds or artificial organs is very complicated. Therefore, it is expected that future investigation will seek to understand the possibility of these more sophisticated technologies being applied for orthopaedic biosensing applications in the near future. After a unique effort by Tatsum and Buttry (1997) [149] on an electrochemical/piezoelectric dual response biosensor, very few investigations have been attempted in this field although it could be a great opportunity to employ a simultaneous multifunctional detector in several advanced biomedical applications. In this context, nontoxic nanocomposite materials can play potential role to improve the performance of immobilized surface modified biosensors. However, focused investigation into homogeneous mixing of nanocomposite materials, particularly at a nano level, is still needed. Therefore, the authors also recommend further research into more ideal base materials that will be perfect as dual-response biosensors or components of multi-response systems simultaneously in the future.

ACKNOWLEDGEMENTS
This study was supported by UM/MOHE/HIR grant (Project number: D000010-16001).

References

1. E. H. Yoo and S. Y. Lee, *Sensors*, 10 (2010) 4558
2. J. S. Schultz, S. Mansouri and I. J. Goldstein, *Diabetes Care*, 5 (1982) 245
3. D. Zhang, Y. Peng, H. Qi, Q. Gao and C. Zhang, *Biosens. Bioelectron.*, 25 (2010) 1088
4. B. Pan, D. Cui, Y. Sheng, C. Ozkan, F. Gao, R. He, Q. Li, P. Xu and T. Huang, *Cancer Res.*, 67 (2007) 8156
5. X. Jia, L. Tan, Q. Xie, Y. Zhang and S. Yao, *Sensor. Actuat. B-Chem.*, 134 (2008) 273
6. J. S. Schultz, *ASAIO trans. Am. Soc. Artif. Intern. Organs*, 32 (1986) 705
7. D. Frense, A. Müller and D. Beckmann, *Sensor. Actuat. B-Chem.*, 51 (1998) 256
8. D. Ivnitski, I. Abdel-Hamid, P. Atanasov and E. Wilkins, *Biosens. Bioelectron.*, 14 (1999) 599
9. S. H. Chen, V. C. H. Wu, Y. C. Chuang and C. S. Lin, *J. Microbiol. Method.*, 73 (2008) 7
10. F. S. Ligler, in *Optical Chemical Sensors.*, C. A. Baldini F, J. Homola and S. Martellucci (Editors), Springer Publisher, USA, 2006, p. 437.
11. B. P. Sagmeister, I. M. Graz, R. Schwödiauer, H. Gruber and S. Bauer, *Biosens. Bioelectron.*, 24 (2009) 2643
12. D. Farrar, J. E. West, I. J. Busch-Vishniac and S. M. Yu, *Scripta Mater.*, 59 (2008) 1051
13. G. Shen, C. Cai and J. Yang, *Electrochim. Acta*, 56 (2011) 8272
14. B. Garipcan, Çağlayan, M.O. and Demirel, G., in *New Perspectives in Biosensors Technology and Applications.*, P. A. Serra (Editors), InTech Publisher, Croatia, 2010, p. 197.
15. T. Vo-Dinh and B. Cullum, *Fresen. J. Anal. Chem.*, 366 (2000) 540

16. J. Wang, *Electroanal.*, 13 (2001) 983
17. A. Mulchandani, W. Chen, P. Mulchandani, J. Wang and K. R. Rogers, *Biosens. Bioelectron.*,16 (2001) 225
18. A. C. R. Grayson, R. S. Shawgo, A. M. Johnson, N. T. Flynn, Y. Li, M. J. Cima and R. Langer, *Proc. IEEE*, 92 (2004) 6
19. D. J. Monk and D. R. Walt, *Anal. Bioanal. Chem.*, 379 (2004) 931
20. J. Wang, *Electroanal.*, 17 (2005) 7
21. S. P. Mohanty and E. Koucianos, *IEEE Potentials*, 25 (2006) 35
22. I. T. Li, E. Pham and K. Truong, *Biotechnol. Lett.*, 28 (2006) 1971
23. W. Mok and Y. Li, *Sensors*, 8 (2008) 7050
24. U. Yogeswaran and S.-M. Chen, *Sensors*, 8 (2008) 290
25. X. Fan, I. M. White, S. I. Shopova, H. Zhu and J. D. Suter, Y. Sun, *Anal. Chim. Acta*, 620 (2008) 8
26. M. Pohanka and P. Skládal, *J. Appl. Biomed.*, 6 (2008) 57
27. X. Zhang, Q. Guo and D. Cui, *Sensors*, 9 (2009) 1033
28. A. N. Reshetilov, Iliasov, P.V., Reshetilova and T.A., in *Intelligent and Biosensors.*, V. S. Somerset(Editors) , InTech Publisher, Croatia, 2010, p. 289.
29. Y. Shao, J. Wang, H. Wu, J. Liu, I. A. Aksay and Y. Lin, *Electroanal.*, 22 (2010) 1027
30. Y. Li, H. J. Schluesener and S. Xu, *Gold Bull.*, 43 (2010) 29
31. A. Kumar M., S. Jung and T. Ji, *Sensors*, 11 (2011) 5087
32. A. Angeli and L. Alessandri, *Gazz. Chim. Ital.*, 46 (1916)
33. W. S. Hughes, *J. Am. Chem. Soc.*, 44 (1922) 2860
34. J. W. Severinghaus and P. B. Astrup, *J. Clin. Monitor.*, 2 (1986) 60
35. L. C. Clark Jr, R. Wolf, D. Granger and Z. Taylor, *J. Appl. Physiol.*, 6 (1953) 189
36. L. C. Clark Jr and C. Lyons, *Ann. NY. Acad. Sci.*, 102 (1962) 29
37. W. H. King Jr, *Anal. Chem.*, 36 (1964) 1735
38. P. Bergveld, *IEEE T. Biomed. Eng.*, BME-17 (1970) 70
39. G. G. Guilbault and G. J. Lubrano, *Anal. Chim. Acta*, 64 (1973) 439
40. N. Opitz and D. W. Lübbers, *Pflug. Arch. Eur. J. Phy.*, 355 (1975) R120
41. G. Kohler and C. Milstein, *Nature*, 256 (1975) 495
42. J. I. Peterson, *Anal. Chem.*, 52 (1980) 864
43. B. Liedberg, C. Nylander and I. Lunström, *Sensor. Actuator.*, 4 (1983) 299
44. A. E. G. Cass, G. Davis, G. D. Francis, H. Allen O Hill, W. J. Aston, I. John Higgins, E. V. Plotkin, L. D. L. Scott and A. P. F. Turner, *Anal. Chem.*, 56 (1984) 667
45. D. R. Matthews, R. R. Holman and E. Bown, *Lancet*, 1 (1987) 778
46. D. R. Coon, A. B. Ogunseitan and G. A. Rechnitz, *Anal. Chem.*, 69 (1997) 4120
47. H. Arwin, *Sensor. Actuat. A-Phys.*, 92 (2001) 43
48. N. C. Shaner, R. E. Campbell, P. A. Steinbach, B. N. G. Giepmans, A. E. Palmer and R. Y. Tsien, *Nat. Biotechnol.*, 22 (2004) 1567
49. N. C. Shaner, P. A. Steinbach and R. Y. Tsien, *Nat. Meth.*, 2 (2005) 905
50. G. Y. Shen, H. Wang, T. Deng, G. L. Shen and R. Q. Yu, *Talanta*, 67 (2005) 217
51. A. M. Smith, S. Dave, S. Nie, L. True and X. Gao, *Expert Rev. Mol. Diagn.*, 6 (2006) 231
52. S. Ghoshal, Mitra, D., Roy, S. and Majumder, D.D., *Sensor. Transd. J.*, 113 (2010) 1
53. P. I. Reyes, C. J. Ku, Z. Duan, Y. Lu, A. Solanki and K. B. Lee, *Appl. Phys. Lett.*, 98 (2011) 173702
54. C. I. L. Justino, T. A. Rocha-Santos and A. C. Duarte, *TrAC – Trend. Anal. Chem.*, 29 (2010) 1172
55. J. K. Jaiswal, H. Mattoussi, J. M. Mauro and S. M. Simon, *Nat. Biotechnol.*, 21 (2003) 47
56. L. Schröder, T. J. Lowery, C. Hilty, D. E. Wemmer and A. Pines, *Science*, 314 (2006) 446
57. O. Taratula and I. J. Dmochowski, *Curr. Opin. Chem. Biol.*, 14 (2010) 97

58. K. E. Mach, P. K. Wong and J. C. Liao, *Trends Pharmacol. Sci.*, 32 (2011) 330
59. S. Y. Niu, S. J. Wang and X. M. Li, *Chinese J. Chem.*, 26 (2008) 134
60. B. Bohunicky and S. A. Mousa, *Nanotech. Sci. Appl.*, 4 (2011) 1
61. N. Vittayakorn and Bongkarn, T., *NU Sci. J.*, 2 (2006) 157
62. Y. Xu (Editors), Elsevier Science Publishers B.V., 1991
63. S. Stolen, E. Bakken and C. E. Mohn, *Phys. Chem. Chem. Phys.*, 8 (2006) 429
64. S.-E. Park and T. R. Shrout, *J. Appl. Phys.*, 82 (1997) 1804
65. G. Sághi-Szabó, R. E. Cohen, H. Krakauer, *Phys. Rev. B*, 59 (1999) 12771
66. M. A. Dubois and P. Muralt, *Sens. Actuat. A-Phys.*, 77 (1999) 106
67. F. Calame and P. Muralt, *Appl. Phys. Lett.*, 90 (2007) 062907
68. P. Muralt, *J. Am. Ceram. Soc.*, 91 (2008) 1385
69. R. E. Cohen, *Nature*, 358 (1992) 136
70. B. Noheda, D. E. Cox, G. Shirane, J. A. Gonzalo, L. E. Cross and S. E. Park, *Appl. Phys. Lett.*, 74 (1999) 2059
71. R. Zachariasz, A. Zarycka and J. Ilczuk, *Mater. Sci.- Poland*, 25 (2007) 781
72. J. Wang, J. B. Neaton and H. Zheng *et al.*, *Science*, 299 (2003) 1719
73. A. Lubk, S. Gemming and N. A. Spaldin, *Phys. Rev. B*, 80 (2009) 104110
74. S. Shanthy and S. K. Singh, *Integr. Ferroelectr.*, 99 (2008) 77
75. X.-Y. Zhang, Q. Song, F. Xu and C. K. Ong, *Appl. Phys. Lett.*, 94 (2009) 022907
76. K. Ujimoto, T. Yoshimura, A. Ashida, N. Fujimura, *Appl. Phys. Lett.*, 100 (2012) 102901
77. A. Manbachi and R. S. C. Cobbold, *Ultrasound*, 19 (2011) 187
78. A. C. Walker, *J. Am. Ceram. Soc.*, 36 (1953) 250
79. Z.-C. Qiu, J.-P. Zhou, G. Zhu, P. Liu and X.-B. Bian, *Bull. Mater. Sci.*, 32 (2009) 193
80. P. Luginbuhl, G. A. Racine, P. Lerch, B. Romanowicz, K. G. Brooks, N. F. de Rooij, P. Renaud and N. Setter, *Sens. Actuat. A-Phys.*, 54 (1996) 530
81. J.-H. Xu, H. Ke, D.-C. Jia, W. Wang and Y. Zhou, *J. Alloy. Compd.*, 472 (2009) 473
82. P. Verardi, M. Dinescu, F. Craciun, R. Dinu, V. Sandu, L. Tapfer and A. Cappello, *Sens. Actuat. A-Phys.*, 74 (1999) 41
83. J. Zhao, L. Lu, C. V. Thompson, Y. F. Lu and W. D. Song, *J. Cryst. Growth*, 225 (2001) 173
84. M. Mahesh Kumar, V. R. Palkar, K. Srinivas and S. V. Suryanarayana, *Appl. Phys. Lett.*, 76 (2000) 2764
85. M. I. S. Veríssimo, P. Q. Mantas, A. M. R. Senos, J. A. B. P. Oliveira and M. T. S. R. Gomes, *Ceram. Int.*, 35 (2009) 617
86. S. Shetty, V. R. Palkar and R. Pinto, *Pramana-J. Phys.*, 58 (2002) 1027
87. S. Ghosh, S. Dasgupta, A. Sen and H. S. Maiti, *Mater. Res. Bull.*, 40 (2005) 2073
88. N. Das, R. Majumdar, A. Sen and H. S. Maiti, *Mater. Lett.*, 61 (2007) 2100
89. C. Z. Tan, T. B. Wang, H. Chen and Z. G. Liu, *Opt. Lett.*, 28 (2003) 1466
90. G. W. Pierce, *Proc. Am. Acad. Arts Sci.*, 59 (1923) 81
91. Y. Qi and M. C. McAlpine, *Energ. Environ. Sci.*, 3 (2010) 1275
92. A. R. Tavakolpour, M. Mailah, I. Z. Mat Darus and O. Tokhi, *Simul. Model. Pract. Th.*, 18 (2010) 516
93. E. M. Hennig, P. R. Cavanagh, H. T. Albert and N. H. Macmillan, *J. Biomed. Eng.*, 4 (1982) 213
94. E. L. May, *J. Therm. Biol.*, 28 (2003) 469
95. G. Song, C. He, Z. Liu, Y. Huang and B. Wu, *Measurement*, 42 (2009) 1214
96. S. Xiong, H. Kawada, H. Yamanaka and T. Matsushima, *Thin Solid Films*, 516 (2008) 5309
97. I. Patel, E. Siores and T. Shah, *Sens. Actuat. A-Phys.*, 159 (2010) 213
98. M. Birkholz, *Z. Phys. B Con. Mat.*, 96 (1995) 333
99. M. W. Hooker (Editors), N. C. F. A. I. (CASI), NASA, USA, 1998, vol. NASA/CR-1998-208708
100. P. Ailertz, *Proc. IRE.*, 49 (1961) 1161

101. Y. Qi, N. T. Jafferis, K. Lyons Jr, C. M. Lee, H. Ahmad and M. C. McAlpine, *Nano Lett.*, 10 (2010) 524
102. R. M. Lec (Editors), Piezoelectric biosensors: Recent advances and applications. Seattle, WA, 2001, p. 419
103. A. I. Kingon and S. Srinivasan, *Nat. Mater.*, 4 (2005) 233
104. J. Ngeh-Ngwainbi, A. A. Suleiman and G. G. Guilbault, *Biosens. Bioelectron.*, 5 (1990) 13
105. G. Sauerbrey, *Z. Phys. A Hadrons Nucl.*, 155 (1959) 206
106. J. Yin, W. Wei, X. Liu, B. Kong, L. Wu and S. Gong, *Anal. Biochem.*, 360 (2007) 99
107. D. Le, F. J. He, T. Jiao Jiang, L. Nie and S. Yao, *J. Microbiol. Meth.*, 23 (1995) 229
108. H. Muramatsu, *Anal. Chem.*, 59 (1987) 2760
109. K. Keiji Kanazawa and J. G. Gordon Ii, *Anal. Chim. Acta*, 175 (1985) 99
110. H. J. Ko and T. H. Park, *Biosens. Bioelectron.*, 20 (2005) 1327
111. X. Lu, Z. Xu, X. Yan, S. Li, W. Ren and Z. Cheng, *Curr. Appl. Phys.*, 11 (2011) S285
112. X. Luo, A. Morrin, A. J. Killard and M. R. Smyth, *Electroanal.*, 18 (2006) 319
113. X. You, R. He, F. Gao, J. Shao, B. Pan and D. Cui, *Nanotechnology*, 18 (2007) 035701
114. B. Pan, D. Cui, P. Xu, Q. Li, T. Huang, R. He and F. Gao, *Colloid. Surface. A*, 295 (2007) 217
115. D. Cui, F. Tian, S. R. Coyer, J. Wang, B. Pan, F. Gao, R. He and Y. Zhang, *J. Nanosci. Nanotechno.*, 7 (2007) 1639
116. F. He, L. Zhang, *Anal. Sci.*, 18 (2002) 397
117. R. J. Martín-Palma, M. Manso and V. Torres-Costa, *Sensors*, 9 (2009) 5149
118. D. A. Krame. US geological survey minerals yearbook—2003. (2003), p. 28.1
119. A. J. Haes and R. P. Van Duyne, *J. Am. Chem. Soc.*, 124 (2002) 10596
120. K. R. Gopidas, J. K. Whitesell and M. A. Fox, *Nano Lett.*, 3 (2003) 1757
121. M. Huang, Y. Shao, X. Sun, H. Chen, B. Liu and S. Dong, *Langmuir*, 21 (2005) 323
122. Y. Ding, J. Liu, H. Wang, G. Shen and R. Yu, *Biomaterials*, 28 (2007) 2147
123. H. Nishikawa, D. Okumura, M. Kusunoki and S. Hontsu, Application of hydroxyapatite thin film as a biosensor. *2006APS..MARV16011N* (2006)
124. R. Ma, B. Wang, Y. Liu, J. Li, Q. Zhao, G. Wang, W. Jia and H. Wang, *Sci. China Ser. B*, 52 (2009) 2013
125. B. Wang, J. J. Zhang, Z. Y. Pan, X. Q. Tao and H. S. Wang, *Biosens. Bioelectron.*, 24 (2009) 1141
126. K. K. Kar and S. Pramanik, I. I. T. Kanpur, USPTO, US 2012/0107612 A1, (2012) p. 32
127. S. Pramanik, Ph.D. thesis, Indian Institute of Technology Kanpur (2011), p. 392
128. S. Pramanik and K. K. Kar, *J. Appl. Poly. Sci.*, 123 (2012) 1100
129. X. C. Zhou, L. Q. Huang and S. F. Y. Li, *Biosens. Bioelectron.*, 16 (2001) 85
130. S. Tombelli, M. Mascini and A. P. F. Turner, *Biosens. Bioelectron.*, 17 (2002) 929
131. A. Bardea, A. Dagan and I. Willner, *Anal. Chim. Acta*, 385 (1999) 33
132. F. Patolsky, A. Lichtenstein and I. Willner, *J. Am. Chem. Soc.*, 122 (2000) 418
133. X. Mao, L. Yang, X. L. Su and Y. Li, *Biosens. Bioelectron.*, 21 (2006) 1178
134. V. Nanduri, I. B. Sorokulova, A. M. Samoylov, A. L. Simonian, V. A. Petrenko and V. Vodyanoy, *Biosens. Bioelectron.*, 22 (2007) 986
135. M. Thust, M. J. Schöning, P. Schroth, U. Malkoc, C. I. Dicker, A. Steffen, P. Kordos and H. Lüth, *J. Mol. Cat. B-Enzym.*, 7 (1999) 77
136. M. Martínez, A. Hilding-Ohlsson, A. A. Viale and E. Cortón, *J. Biochem. Biophys. Meth.*, 70 (2007) 455
137. L. Chen and G. Lu, *Sensor. Actuat. B-Chem.*, 121 (2007) 423
138. S. Chinnayelka and M. J. McShane, *Anal. Chem.*, 77 (2005) 5501
139. R. Gupta and N. K. Chaudhury, *Biosens. Bioelectron.*, 22 (2007) 2387
140. M. Sriyudthsak, H. Yamagishi and T. Moriizumi, *Thin Solid Films*, 160 (1988) 463
141. S. Cosnier, *Electroanal.*, 9 (1997) 894

142. A. Ottova, V. Tvarozek, J. Racek, J. Sabo, W. Ziegler, T. Hianik and H. T. Tien, *Supramol. Sci.*, 4 (1997) 101
143. S. Rodriguez-Mozaz, M. P. Marco, M. J. Lopez De Alda and D. Barceló, *Pure Appl. Chem.*, 76 (2004) 723
144. S. Babacan, P. Pivarnik, S. Letcher and A. G. Rand, *Biosens. Bioelectron.*, 15 (2000) 615
145. S. Tombelli, M. Mascini, L. Braccini, M. Anichini and A. P. F. Turner, *Biosens. Bioelectron.*, 15 (2000) 363
146. J. Y. Yang, Y. Li, S. M. Chen and K. C. Lin, *Int. J. Electrochem. Sci.*, 6 (2011) 2223
147. S. Egusa, Z. Wang, N. Chocat *et al.*, *Nat. Mater.*, 9 (2010) 643
148. S. Pramanik, B. Pingguan-Murphy and N. A. Abu Osman, *Sci. Tech. Adv. Mater.*, 13 (2012) 043002
149. T. Tatsuma and D. A. Buttry, *Anal. Chem.*, 69 (1997) 887